Main manuscript

Title

Evolution of the potassium channel gene *Kcnj13* underlies colour pattern diversification in *Danio* fish

Authors

Marco Podobnik

marco.podobnik@tuebingen.mpg.de

https://orcid.org/0000-0001-5480-7086

Hans Georg Frohnhöfer

hans-georg.frohnhoefer@tuebingen.mpg.de

https://orcid.org/0000-0003-4038-7089

Christopher M. Dooley

christopher.dooley@tuebingen.mpg.de

https://orcid.org/0000-0002-4941-9019

Anastasia Eskova

anastasia.eskova@ibm.com

https://orcid.org/0000-0002-4599-2109

Christiane Nüsslein-Volhard

christiane.nuesslein-volhard@tuebingen.mpg.de

https://orcid.org/0000-0002-7688-1401

Uwe Irion

uwe.irion@tuebingen.mpg.de

https://orcid.org/0000-0003-2823-5840

Abstract

The genetic basis of morphological variation provides a major topic in evolutionary biology[1-6]. Colour patterns in fish are among the most diverse of all vertebrates. Species of the genus *Danio* display strikingly different colour patterns ranging from horizontal stripes, to vertical bars or spots[7-10]. Stripe formation in zebrafish, *Danio rerio*, oriented by the horizontal myoseptum, is a self-organizing process based on cell-contact-mediated interactions between three types of chromatophores with a leading role of iridophores[11-14]. We investigated genes known to regulate chromatophore interactions in zebrafish as candidates that might have evolved to produce a pattern of vertical bars in its sibling species, *Danio aesculapii*[8,10]. Using gene editing[15-17] we generated several mutants in *D. aesculapii* that demonstrate a lower complexity in the interactions between chromatophores in this species, as well as a minor role of iridophores in patterning. Complementation tests in interspecific hybrids[18,19] identified *obelix/Kcnj13*, which encodes an inwardly rectifying potassium channel (Kir7.1)[20], as a gene evolved between *D. rerio* and *D. aesculapii* as well as in two of seven more *Danio* species tested. Our results demonstrate that the CRISPR/Cas9-system allows straightforward genetic tests also in non-model vertebrates to identify genes that underlie morphological evolution.

Main

Colour patterns are common features of animals and have important functions in camouflage, as signals for kin recognition, or mate choice. As targets for natural and sexual selection, they are of high evolutionary significance[21-24]. The zebrafish, *Danio rerio*, has emerged as a model system to study colour pattern development in a vertebrate[14,25-29]. A fair number of genes have been identified that are required for the formation of the pattern[28,29], which is composed of a series of horizontal light and dark stripes on the flank of the fish as well as in the anal and tail fins (Fig. 1a). The adult pattern is created by three different types of pigment cells (chromatophores) in the skin, black melanophores, blue or silvery iridophores and yellow xanthophores[13,30-32]. The chromatophores producing this pattern mainly originate

from multipotent neural crest–derived stem cells located at the dorsal root ganglia of the peripheral nervous system[33-37]. Signalling pathways, e.g. Csf1 or Edn3, control proliferation and spreading of chromatophores[38-40]. During metamorphosis, the period when adult form and colour pattern are established, assembly into the striped pattern is controlled by interactions between the three cell types. Several genes are autonomously required in the chromatophores for these heterotypic interactions[11,12,20,41-43]. These genes typically encode integral membrane proteins such as adhesion molecules[42], channels[20], or components of cellular junctions, some of which mediate direct cell contacts[43,44]. In *Meox1* (*choker*) mutants, lacking the horizontal myoseptum as anatomical landmark, the horizontal orientation is lost, but stripes form of normal width and composition (Fig. 1b), indicating that stripe formation is a process of self-organization of the pigment cells[11].

Danio species show an amazing variety of colour patterns, which range from horizontal stripes in *D. rerio* (Fig. 1a), over vertical bars in *D. aesculapii*, *D. choprae* or *D. erythromicron* (Fig. 1c, g, m) to spotted patterns in *D. tinwini* or *D. margaritatus* (Fig. 1d, h). The *Danio* species diversified for at least 13 million years in Southeast Asia and their spatial distributions only partially overlap today[10,45]. Hybrids between *D. rerio* and other *Danio* species can be produced in the laboratory by natural matings or by *in vitro* fertilization[19]. They invariably display colour patterns similar to the stripes in *D. rerio*, thus, horizontal stripes appear to be dominant over divergent patterns (Fig. 1e, f, i, j)[19]; whether this is due to a gain-of-function in striped species or losses in the other species is an open question[25,28,29]. The hybrids are virtually sterile impeding further genetic experiments, like QTL mapping, but they allow interspecific complementation tests[19]. Using this approach, we identified the potassium channel gene *Kcnj13* as repeatedly evolved in the *Danio* genus.

Prevalent pattern orientation by the horizontal myoseptum

To reconstruct the history of colour pattern evolution we first investigated how pattern orientation is inherited in hybrids (see phylogenetic relationships depicted on the left of Fig. 4). The horizontal orientation of the stripes in *D. rerio* depends on the horizontal myoseptum (Fig. 1a, b)[11,13]. The closest sibling species to *D. rerio*,

D. aesculapii, shows a very different pattern of vertically oriented dark bars (Fig. 1c)[8]. Similar barred patterns are exhibited by the more distantly related *D. choprae* and *D. erythromicron* (Fig. 1g, m). These patterns clearly do not use the horizontal myoseptum for orientation. In all three cases, hybrids with *D. rerio* show a pattern that resembles the horizontal *D. rerio* stripes (Fig. 1e, i, n)[29]. Strikingly, hybrids between *D. aesculapii* and *D. choprae* display a barred pattern (Fig. 1k). This indicates that the cues for horizontal orientation are lacking and that the pattern develops in a similar manner in both barred species. In contrast, hybrids between *D. aesculapii* and *D. erythromicron* develop highly variable patterns without any clear orientation (Fig. 1o; Extended Data Fig. 1). Therefore, the vertical bars must develop in a different manner in *D. erythromicron* compared to *D. aesculapii* and *D. choprae*.

Two *Danio* species display spotted patterns: *D. tinwini* has dark spots on a light background (Fig. 1d)[9], whereas *D. margaritatus* shows light spots on a dark background (Fig. 1h)[7]. In both cases, hybrids with *D. rerio* show a stripe pattern similar to *D. rerio* (Fig. 1f, j)[29]. Hybrids between the two spotted species also develop a pattern of horizontal stripes, albeit with some interruptions and irregularities (Fig. 1l). These results indicate that the horizontal myoseptum functions to orient the pattern in the hybrids between *D. tinwini* and *D. margaritatus*, and therefore in at least one of the two parental species. It seems likely that this is the case in *D. tinwini*, as the spots show some horizontal orientation reminiscent of interrupted stripes. Hybrids between *D. aesculapii* and *D. margaritatus* develop meandering patterns that do not resemble either of the parental species and lack a clear horizontal or vertical orientation (Fig. 1p). Based on the most recent phylogeny[10], we hypothesize an evolutionary history, in which the horizontal orientation of the pattern in the *D. rerio* group was gained from an ancestral ambiguous pattern and lost again in *D. aesculapii.* Two other species, *D. erythromicron* and *D. choprae,* independently might have acquired a vertical orientation from this ancestral pattern. The patterns of the hybrids between *D. aesculapii* and *D. erythromicron* or *D. margaritatus*, which are without clear orientation, might resemble such an ancestral pattern. These patterns are much more variable than the species patterns (Extended Data Fig. 1) suggesting that the ancestral patterns did not function as recognition signals but rather provided camouflage.

Chromatophore interactions in stripes and bars

To investigate the developmental and genetic basis for the differences in pattern formation, we focussed on the sibling species *D. rerio* and *D. aesculapii*, which display horizontal stripes and vertical bars, respectively (Fig. 1a, c). In *D. rerio,* during early metamorphosis, iridophores emerge along the horizontal myoseptum to form the first light stripe (Extended Data Fig. 2a)[11-13]. In contrast, in *D. aesculapii* iridophores appear more scattered over the flank and only during later stages (Extended Data Fig. 2b, d). This indicates that it is not the physical presence of the horizontal myoseptum, which exists in both species, but specific guidance signals directing the cells into the skin in *D. rerio*, which lack in *D. aesculapii*. Later, when iridophores, covered by compact xanthophores, have formed the first contiguous light stripe with adjacent melanophore stripes in *D. rerio* (Extended Data Fig. 2c, e), in *D. aesculapii* melanophores and xanthophores intermix broadly (Extended Data Fig. 2f); they sort out loosely into vertical bars of low contrast without coherent sheets of dense iridophores between the melanophore bars during later stages (Extended Data Fig. 2h). Our observations suggest that the different patterns in these sibling species are produced by the presence or absence of guidance signals for iridophores along the horizontal myoseptum as well as by cellular interactions that prevent mixing of melanophores and xanthophores in *D. rerio* but not in *D. aesculapii*.

To address the role of the different cell types, we used the CRISPR/Cas9 system to generate mutants lacking individual chromatophore types in *D. aesculapii*. Whereas in *D. rerio* vestiges of the striped pattern form in the absence of one chromatophore type (Fig. 2a, b, c)[11], loss of either melanophores (Fig. 2d) or xanthophores (Fig. 2e) completely abolishes the patterning in *D. aesculapii*. This indicates that the repulsive interactions between melanophores or xanthophores and iridophores, which account for the residual patterns in *D. rerio*[11,12], are absent in *D. aesculapii*. In contrast, eliminating iridophores in *D. aesculapii* still permits some melanophore bar formation (Fig. 2f). This indicates that iridophores, which play a dominant role for stripe

158 formation in *D. rerio*, are dispensable for the formation of vertical bars in
159 *D. aesculapii*.

160

161 Next, we analysed genes with known functions in heterotypic interactions between
162 chromatophores. In *D. rerio* loss-of-function mutations in the gap junction genes
163 *Cx39.4* (*luchs*)[44,46] and *Cx41.8/Gja5b* (*leopard*)[41,46,47] as well as mutations in *Igsf11*
164 (*seurat*)[42], which codes for a cell adhesion molecule, lead to melanophore spots (Fig.
165 2j, Extended Data Fig. 3a, c, e), whereas mutations in *Kir7.1/Kcnj13* (*obelix*/*jaguar*)
166 result in fewer and wider stripes with some mixing of melanophores and
167 xanthophores (Fig. 2g)[20,48]. So far, only dominant alleles of *Kcnj13* have been
168 described[41,46,49]. We used the CRISPR/Cas9 system to generate a *Kcnj13* loss-of-
169 function allele in *D. rerio*, which is recessive (Fig. 2h, Extended Data Fig. 3e, g,
170 Supplementary Information). To investigate the functions of these four genes in
171 *D. aesculapii*, we generated mutants in the orthologs. In all of them we find an even
172 distribution of melanophores (Fig. 2i, Extended Data Fig. 3b, d, f, h) indicating that
173 the interactions mediated by these genes are essential to generate the melanophore
174 bars in *D. aesculapii*. The complete loss of a pattern in single mutants in *D.*
175 *aesculapii* is different from *D. rerio* where this occurs only in double mutants
176 (Fig. 2k)[46]. In concert with predictions of agent-based models of patterning[50], this
177 indicates that the robust formation of horizontal stripes in *D. rerio* is due to a gain in
178 complexity based on partially redundant chromatophore interactions. These are
179 dominated by iridophores and oriented by an as yet unidentified signal along the
180 horizontal myoseptum. *D. aesculapii* might have secondarily lost the dominance of
181 iridophores leading to a pattern based primarily on interactions between
182 xanthophores and melanophores and thus of lower complexity.

183

184 The ability to generate loss-of-function mutations in both species allowed us to
185 generate interspecific hybrids, which carry loss-of-function alleles from both parental
186 species. These hybrids are very similar to the respective *D. rerio* mutants (Fig. 2l,
187 Extended Data Fig. 3i, j), indicating that these genes have the same functions during
188 stripe formation in *D. rerio* and the hybrids.

189

***Kcnj13* evolved repeatedly in the *Danio* genus**

Next, we generated reciprocal heterozygotes, i.e. interspecific hybrids carrying a loss-of-function allele from either one of the parental species in an otherwise identical genetic background[18]. This powerful genetic test to identify evolved genes has not been applied in vertebrates, so far. We expect similar patterns in these hybrids if the gene function can be fully provided by either wild-type allele. A qualitatively altered hybrid pattern would reveal that one of the wild-type alleles cannot complement the loss-of-function of the other, therefore indicating functional changes during evolution. We found that heterozygous hybrids with the loss-of-function allele of *Kcnj13* from *D. rerio* display a pattern of spots or interrupted stripes whereas a striped pattern forms with the mutant allele from *D. aesculapii* (Fig. 3a, b, Extended Data Fig. 4g, h). This indicates that the wild-type allele from *D. aesculapii* cannot compensate for the loss of the *D. rerio* allele. In contrast, in the case of heterozygous hybrids with *Cx39.4*, *Cx41.8* and *Igsf11* striped patterns indistinguishable from wild-type hybrids are formed regardless whether the wild-type allele stems from *D. rerio* (Extended Data Fig. 4b, d, f) or the other species (Extended Data Fig. 4a, c, e). These reciprocal heterozygosity tests indicate that *Cx39.4*, *Cx41.8* and *Igsf11* provide similar functions in both species, whereas the function of *Kcnj13* has evolved between the two species.

To investigate if *Kcnj13* underlies the pattern variation more broadly across the *Danio* genus, we tested seven additional species (Fig. 4a, top to bottom). As mentioned above, wild-type hybrids between *D. rerio* and all other *Danio* species display horizontal stripes, resembling the *D. rerio* pattern, with slight defects in *D. albolineatus* (Fig. 4b). Strikingly, not only *D. rerio Kcnj13* k.o. / *D. aesculapii* hybrids (Fig. 4c, highlighted in magenta) but also *D. rerio Kcnj13* k.o. / *D. tinwini* hybrids developed patterns of spots or interrupted stripes indicating that the *Kcnj13* function must have evolved compared to *D. rerio* (Fig. 4c, highlighted in yellow). This pattern, which is qualitatively different from all wild-type hybrids and also from the *D. rerio Kcnj13* mutant pattern, is similar to the parental pattern of *D. tinwini*, where dense iridophores interrupt the dark melanophore stripes (Fig. 1d, Fig. 4c). *D. rerio Kcnj13* k.o. / *D. choprae* hybrids also developed patterns that resemble interrupted

stripes (Fig. 4c, highlighted in cyan), similar to the *D. rerio Kcnj13* k.o. / *D. aesculapii* hybrid pattern (Fig. 4c). No qualitative differences were detected between wild-type hybrids (Fig. 4b) and hybrids heterozygous for *D. rerio Kcnj13* in the case of *D. kyathit*, *D. nigrofasciatus*, *D. albolineatus*, *D. erythromicron* and *D. margaritatus* (Fig. 4c). This indicates that the alleles from these species complement the loss of the *D. rerio Kcnj13* allele. Functional changes of *Kcnj13* occurred in *D. aesculapii*, *D. tinwini* and *D. choprae* compared to *D. rerio*, however, heterozygous hybrids did not develop pure *D. rerio Kcnj13* mutant patterns indicating that the orthologs still provide some function for patterning across all species tested. The separated positions of the three species with the different functions of *Kcnj13* in the phylogenetic tree (graph on the left of Fig. 4)[10] indicate a repeated and independent evolution of the same gene.

Kcnj13

Potassium channels have important roles in tissue patterning[51], notably in the regulation of allometric growth of fins in *D. rerio*[52,53]. *Kcnj13* encodes an inwardly rectifying potassium channel (Kir7.1) conserved in vertebrates (Extended Data Fig. 5). Mutations are known to cause defects in tracheal development in mice[54] and two rare diseases in humans leading to visual impairment[54-60]. During colour pattern formation in *D. rerio* its function is autonomously required in melanophores[48], and in *ex vivo* studies it was shown that the channel is involved in the contact-dependent depolarisation of melanophores upon interaction with xanthophores leading to a repulsion between these cells[43]. Evolution in *Kcnj13* in *D. aesculapii*, *D. tinwini* and *D. choprae* might therefore cause differences in heterotypic chromatophore interactions between species. The protein coding sequences of *Kcnj13* orthologs are highly conserved in all *Danio* species with only very few diverged sites in the cytoplasmic N- and C-terminal parts of the protein (Extended Data Fig. 6). Whether any of these amino acid changes might affect the function of the channel and/or if changes in gene expression are the basis for the repeated evolution of *Kcnj13* will require further experiments.

In contrast to mammals and birds, basal vertebrates retained several chromatophore types providing a substrate for the development of elaborate colour patterns. Their rapid and extensive evolutionary diversification is most likely if the number of underlying genes is small[61]. Several patterning genes have been repeatedly identified in genetic screens in *D. rerio*[41,46,49]. These genes provide candidates that might have evolved to contribute to patterning differences between *Danio* species. Evolved genes have been identified in *D. albolineatus* and *D. nigrofasciatus*, where changes in two signalling pathways, Csf1 or Edn3, likely underlie patterning variations by differentially promoting xanthophore or iridophore development, respectively[19,36,62]. We focused on genes regulating heterotypic interactions between chromatophores as a potential genetic basis for colour pattern evolution. Using interspecific mutant complementation tests we identified the potassium channel gene *Kcnj13* as contributing to patterning divergence in multiple *Danio* species. We have shown that this genus offers the opportunity to identify evolved genes and to reconstruct the evolution of biodiversity.

Main Text References

1 Sucena, E. & Stern, D. L. Divergence of larval morphology between Drosophila sechellia and its sibling species caused by cis-regulatory evolution of ovo/shaven-baby. *Proceedings of the National Academy of Sciences of the United States of America* **97**, 4530-4534, doi:10.1073/pnas.97.9.4530 (2000).

2 Colosimo, P. F. *et al.* Widespread parallel evolution in sticklebacks by repeated fixation of Ectodysplasin alleles. *Science* **307**, 1928-1933, doi:10.1126/science.1107239 (2005).

3 Westerman, E. L. *et al.* Aristaless Controls Butterfly Wing Color Variation Used in Mimicry and Mate Choice. *Curr Biol* **28**, 3469-3474 e3464, doi:10.1016/j.cub.2018.08.051 (2018).

4 Barrett, R. D. H. *et al.* Linking a mutation to survival in wild mice. *Science* **363**, 499-504, doi:10.1126/science.aav3824 (2019).

5 Hu, Y., Linz, D. M. & Moczek, A. P. Beetle horns evolved from wing serial homologs. *Science* **366**, 1004-1007, doi:10.1126/science.aaw2980 (2019).

6 Orteu, A. & Jiggins, C. D. The genomics of coloration provides insights into adaptive evolution. *Nat Rev Genet*, doi:10.1038/s41576-020-0234-z (2020).

7 Roberts, T. R. The 'celestial pearl danio', a new genus and species of colourful minute cyprinid fish from Myanmar (Pisces: Cypriniformes). *Raffles Bulletin of Zoology* **55**, 131-140 (2007).

8 Kullander, S. O. & Fang, F. Danio aesculapii, a new species of danio from south-western Myanmar (Teleostei: Cyprinidae). *Zootaxa* **2164**, 41-48 (2009).

9 Kullander, S. O. & Fang, F. Danio tinwini, a new species of spotted danio from northern Myanmar (Teleostei: Cyprinidae). *Ichthyological Exploration of Freshwaters* **20**, 223-228 (2009).

10 McCluskey, B. M. & Postlethwait, J. H. Phylogeny of zebrafish, a "model species," within Danio, a "model genus". *Mol Biol Evol* **32**, 635-652, doi:10.1093/molbev/msu325 (2015).

11 Frohnhöfer, H. G., Krauss, J., Maischein, H. M. & Nüsslein-Volhard, C. Iridophores and their interactions with other chromatophores are required for stripe formation in zebrafish. *Development* **140**, 2997-3007, doi:10.1242/dev.096719 (2013).

12 Patterson, L. B. & Parichy, D. M. Interactions with iridophores and the tissue environment required for patterning melanophores and xanthophores during zebrafish adult pigment stripe formation. *PLoS genetics* **9**, e1003561, doi:10.1371/journal.pgen.1003561 (2013).

13 Singh, A. P., Schach, U. & Nüsslein-Volhard, C. Proliferation, dispersal and patterned aggregation of iridophores in the skin prefigure striped colouration of zebrafish. *Nature cell biology* **16**, 607-614, doi:10.1038/ncb2955 (2014).

14 Irion, U., Singh, A. P. & Nüsslein-Volhard, C. in *Current Topics in Developmental Biology* Ch. 8, (Elsevier Inc., 2016).

15 Jinek, M. *et al.* A programmable dual-RNA-guided DNA endonuclease in adaptive bacterial immunity. *Science* **337**, 816-821, doi:10.1126/science.1225829 (2012).

16 Hwang, W. Y. *et al.* Heritable and precise zebrafish genome editing using a CRISPR-Cas system. *PloS one* **8**, e68708, doi:10.1371/journal.pone.0068708 (2013).

17 Irion, U., Krauss, J. & Nüsslein-Volhard, C. Precise and efficient genome editing in zebrafish using the CRISPR/Cas9 system. *Development* **141**, 4827-4830, doi:10.1242/dev.115584 (2014).

18 Stern, D. L. Identification of loci that cause phenotypic variation in diverse species with the reciprocal hemizygosity test. *Trends Genet* **30**, 547-554, doi:10.1016/j.tig.2014.09.006 (2014).

19 Parichy, D. M. & Johnson, S. L. Zebrafish hybrids suggest genetic mechanisms for pigment pattern diversification in Danio. *Development genes and evolution* **211**, 319-328 (2001).

20 Iwashita, M. *et al.* Pigment pattern in jaguar/obelix zebrafish is caused by a Kir7.1 mutation: implications for the regulation of melanosome movement. *PLoS genetics* **2**, e197, doi:10.1371/journal.pgen.0020197 (2006).

21 Darwin, C. The Descent of Man, and Selection in Relation to Sex. *John Murray, London.* (1871).

22 Protas, M. E. & Patel, N. H. Evolution of coloration patterns. *Annu Rev Cell Dev Biol* **24**, 425-446, doi:10.1146/annurev.cellbio.24.110707.175302 (2008).

23 Cuthill, I. C. *et al.* The biology of color. *Science* **357**, doi:10.1126/science.aan0221 (2017).

24 Nüsslein-Volhard, C., Grutzmacher, S. & Howard, J. *Animal beauty : on the evolution of biological aesthetics*. (The MIT Press, 2019).

25 Parichy, D. M. Evolution of danio pigment pattern development. *Heredity* **97**, 200-210, doi:10.1038/sj.hdy.6800867 (2006).

26 Kondo, S., Iwashita, M. & Yamaguchi, M. How animals get their skin patterns: fish pigment pattern as a live Turing wave. *Int J Dev Biol* **53**, 851-856, doi:10.1387/ijdb.072502sk (2009).

27 Singh, A. P. & Nüsslein-Volhard, C. Zebrafish stripes as a model for vertebrate colour pattern formation. *Curr Biol* **25**, R81-92, doi:10.1016/j.cub.2014.11.013 (2015).

28 Irion, U. & Nüsslein-Volhard, C. The identification of genes involved in the evolution of color patterns in fish. *Curr Opin Genet Dev* **57**, 31-38, doi:10.1016/j.gde.2019.07.002 (2019).

29 Patterson, L. B. & Parichy, D. M. Zebrafish Pigment Pattern Formation: Insights into the Development and Evolution of Adult Form. *Annu Rev Genet* **53**, 505-530, doi:10.1146/annurev-genet-112618-043741 (2019).

30 Hirata, M., Nakamura, K., Kanemaru, T., Shibata, Y. & Kondo, S. Pigment cell organization in the hypodermis of zebrafish. *Developmental dynamics : an official publication of the American Association of Anatomists* **227**, 497-503, doi:10.1002/dvdy.10334 (2003).

31 Hirata, M., Nakamura, K. & Kondo, S. Pigment cell distributions in different tissues of the zebrafish, with special reference to the striped pigment pattern. *Developmental dynamics : an official publication of the American Association of Anatomists* **234**, 293-300, doi:10.1002/dvdy.20513 (2005).

32 Mahalwar, P., Walderich, B., Singh, A. P. & Nüsslein-Volhard, C. Local reorganization of xanthophores fine-tunes and colors the striped pattern of zebrafish. *Science* **345**, 1362-1364, doi:10.1126/science.1254837 (2014).

33 Budi, E. H., Patterson, L. B. & Parichy, D. M. Post-embryonic nerve-associated precursors to adult pigment cells: genetic requirements and dynamics of morphogenesis and differentiation. *PLoS genetics* **7**, e1002044, doi:10.1371/journal.pgen.1002044 (2011).

34 Mongera, A. *et al.* Genetic lineage labeling in zebrafish uncovers novel neural crest contributions to the head, including gill pillar cells. *Development* **140**, 916-925, doi:10.1242/dev.091066 (2013).

35 Dooley, C. M., Mongera, A., Walderich, B. & Nusslein-Volhard, C. On the embryonic origin of adult melanophores: the role of ErbB and Kit signalling in establishing melanophore stem cells in zebrafish. *Development* **140**, 1003-1013, doi:10.1242/dev.087007 (2013).

36 Patterson, L. B., Bain, E. J. & Parichy, D. M. Pigment cell interactions and differential xanthophore recruitment underlying zebrafish stripe reiteration and Danio pattern evolution. *Nature communications* **5**, 5299, doi:10.1038/ncomms6299 (2014).

37 Singh, A. P. *et al.* Pigment Cell Progenitors in Zebrafish Remain Multipotent through Metamorphosis. *Dev Cell* **38**, 316-330, doi:10.1016/j.devcel.2016.06.020 (2016).

38 Parichy, D. M. *et al.* Mutational analysis of endothelin receptor b1 (rose) during neural crest and pigment pattern development in the zebrafish Danio rerio. *Developmental biology* **227**, 294-306, doi:10.1006/dbio.2000.9899 (2000).

383 39 Parichy, D. M. & Turner, J. M. Temporal and cellular requirements for Fms
384 signaling during zebrafish adult pigment pattern development. *Development*
385 **130**, 817-833 (2003).
386 40 Walderich, B., Singh, A. P., Mahalwar, P. & Nusslein-Volhard, C. Homotypic
387 cell competition regulates proliferation and tiling of zebrafish pigment cells
388 during colour pattern formation. *Nat Commun* **7**, 11462,
389 doi:10.1038/ncomms11462 (2016).
390 41 Haffter, P. *et al.* Mutations affecting pigmentation and shape of the adult
391 zebrafish. *Development genes and evolution* **206**, 260-276, doi:DOI
392 10.1007/s004270050051 (1996).
393 42 Eom, D. S. *et al.* Melanophore migration and survival during zebrafish adult
394 pigment stripe development require the immunoglobulin superfamily adhesion
395 molecule Igsf11. *PLoS genetics* **8**, e1002899,
396 doi:10.1371/journal.pgen.1002899 (2012).
397 43 Inaba, M., Yamanaka, H. & Kondo, S. Pigment pattern formation by contact-
398 dependent depolarization. *Science* **335**, 677, doi:10.1126/science.1212821
399 (2012).
400 44 Watanabe, M., Sawada, R., Aramaki, T., Skerrett, I. M. & Kondo, S. The
401 Physiological Characterization of Connexin41.8 and Connexin39.4, Which Are
402 Involved in the Striped Pattern Formation of Zebrafish. *J Biol Chem* **291**,
403 1053-1063, doi:10.1074/jbc.M115.673129 (2016).
404 45 Parichy, D. M. Advancing biology through a deeper understanding of
405 zebrafish ecology and evolution. *Elife* **4**, doi:10.7554/eLife.05635 (2015).
406 46 Irion, U. *et al.* Gap junctions composed of connexins 41.8 and 39.4 are
407 essential for colour pattern formation in zebrafish. *Elife* **3**, e05125,
408 doi:10.7554/eLife.05125 (2014).
409 47 Watanabe, M. *et al.* Spot pattern of leopard Danio is caused by mutation in
410 the zebrafish connexin41.8 gene. *EMBO reports* **7**, 893-897,
411 doi:10.1038/sj.embor.7400757 (2006).
412 48 Maderspacher, F. & Nüsslein-Volhard, C. Formation of the adult pigment
413 pattern in zebrafish requires leopard and obelix dependent cell interactions.
414 *Development* **130**, 3447-3457 (2003).

49 Henke, K. *et al.* Genetic Screen for Postembryonic Development in the Zebrafish (Danio rerio): Dominant Mutations Affecting Adult Form. *Genetics* **207**, 609-623, doi:10.1534/genetics.117.300187 (2017).

50 Volkening, A. & Sandstede, B. Iridophores as a source of robustness in zebrafish stripes and variability in Danio patterns. *Nat Commun* **9**, 3231, doi:10.1038/s41467-018-05629-z (2018).

51 Dahal, G. R. *et al.* An inwardly rectifying K+ channel is required for patterning. *Development* **139**, 3653-3664, doi:10.1242/dev.078592 (2012).

52 Perathoner, S. *et al.* Bioelectric signaling regulates size in zebrafish fins. *PLoS genetics* **10**, e1004080, doi:10.1371/journal.pgen.1004080 (2014).

53 Stewart, S. *et al.* longfin causes cis-ectopic expression of the kcnh2a ether-a-go-go K^+ channel to autonomously prolong fin outgrowth. *bioRxiv*, 790329, doi:10.1101/790329 (2019).

54 Lee, M. M., Ritter, R., 3rd, Hirose, T., Vu, C. D. & Edwards, A. O. Snowflake vitreoretinal degeneration: follow-up of the original family. *Ophthalmology* **110**, 2418-2426, doi:10.1016/S0161-6420(03)00828-5 (2003).

55 Hejtmancik, J. F. *et al.* Mutations in KCNJ13 cause autosomal-dominant snowflake vitreoretinal degeneration. *Am J Hum Genet* **82**, 174-180, doi:10.1016/j.ajhg.2007.08.002 (2008).

56 Sergouniotis, P. I. *et al.* Recessive mutations in KCNJ13, encoding an inwardly rectifying potassium channel subunit, cause leber congenital amaurosis. *Am J Hum Genet* **89**, 183-190, doi:10.1016/j.ajhg.2011.06.002 (2011).

57 Khan, A. O., Bergmann, C., Neuhaus, C. & Bolz, H. J. A distinct vitreo-retinal dystrophy with early-onset cataract from recessive KCNJ13 mutations. *Ophthalmic Genet* **36**, 79-84, doi:10.3109/13816810.2014.985846 (2015).

58 Pattnaik, B. R. *et al.* A Novel KCNJ13 Nonsense Mutation and Loss of Kir7.1 Channel Function Causes Leber Congenital Amaurosis (LCA16). *Hum Mutat* **36**, 720-727, doi:10.1002/humu.22807 (2015).

59 Perez-Roustit, S. *et al.* Leber Congenital Amaurosis with Large Retinal Pigment Clumps Caused by Compound Heterozygous Mutations in Kcnj13. *Retin Cases Brief Rep* **11**, 221-226, doi:10.1097/ICB.0000000000000326 (2017).

449 60 Toms, M. *et al.* Missense variants in the conserved transmembrane M2
450 protein domain of KCNJ13 associated with retinovascular changes in humans
451 and zebrafish. *Exp Eye Res* **189**, 107852, doi:10.1016/j.exer.2019.107852
452 (2019).
453 61 Gavrilets, S. & Losos, J. B. Adaptive radiation: contrasting theory with data.
454 *Science* **323**, 732-737, doi:10.1126/science.1157966 (2009).
455 62 Spiewak, J. E. *et al.* Evolution of Endothelin signaling and diversification of
456 adult pigment pattern in Danio fishes. *PLoS genetics* **14**, e1007538,
457 doi:10.1371/journal.pgen.1007538 (2018).
458

Methods

No statistical methods were used to predetermine sample size. The experiments were not randomized. The investigators were not blinded to allocation during experiments and outcome assessment.

Fish husbandry

Zebrafish, *D. rerio*, were maintained as described earlier[1]. If not newly generated (Table 4, Supplementary Information), the following genotypes were used: wild-type Tuebingen/TU, *nacre*^{w2}*/nac/Mitfa*[2], *pfeffer*^{tm236}*/pfe/Csf1ra*[3], *transparent*^{b6}*/tra/Mpv17*[4], *leopard*^{t1}*/leo/Cx41.8*[5,6], *luchs*^{t37ui}*/luc/Cx39.4*[7], *obelix*^{tXG6}*/obe/Kcnj13*[7].

D. aesculapii and *D. albolineatus* were treated identical to *D. rerio*. For the other *Danio* species, *D. kyathit*, *D. tinwini*, *D. nigrofasciatus*, *D. choprae*, *D. margaritatus* and *D. erythromicron* individual pair matings were not successful. Therefore, the fish were kept in groups in tanks containing boxes lightly covered with Java moss (*Taxiphyllum barbieri*), which resulted in sporadic matings and allowed us to collect fertilized eggs.

Interspecific hybrids were either obtained by natural matings or by in vitro fertilizations[8]. Heterozygous or trans-heterozygous mutant hybrids were identified by PCR and sequence analysis using specific primer pairs (Table 1 and 3, Supplementary Information).

All species were staged according to the normal table of *D. rerio* development[9]. All animal experiments were performed in accordance with the rules of the State of Baden-Württemberg, Germany, and approved by the Regierungspräsidium Tübingen.

CRISPR/Cas9 gene editing

The CRISPR/Cas9 system was applied either as described in[10] or according to the guidelines for embryo microinjection of IDT. Briefly, oligonucleotides were cloned into pDR274 to generate the sgRNA vector (Table 2, Supplementary Information). sgRNAs were transcribed from the linearized vector using the MEGAscript T7

Transcription Kit (Invitrogen). Alternatively, target-specific crRNAs and universal tracrRNAs were purchased from IDT. sgRNAs or crRNA:tracrRNA duplexes were injected as ribonucleoprotein complexes with Cas9 proteins into one-cell stage embryos. The efficiency of indel generation was tested on eight larvae at 1 dpf by PCR using specific primer pairs and by sequence analysis as described previously (Table 1 and 3, Supplementary Information)[11]. The remaining larvae were raised to adulthood. Mature F0 fish carrying indels were outcrossed. Loss-of-function alleles in heterozygous F1 fish were selected to establish homozygous or trans-heterozygous mutant lines (Table 4, Supplementary Information).

Image acquisition

Anesthesia of adult fish was performed as described previously[11]. A Canon 5D Mk II camera was used to obtain images. Juvenile fish were either embedded in low melting point agarose or fixed in 4% formaldehyde/0.08% glutaraldehyde and then photographed under a Leica MZ1 stereomicroscope (Extended Data Fig. 2). Images were processed using Fiji[12], Adobe Photoshop and Adobe Illustrator CS6.

RNA-Sequencing and transcriptome analysis

Skin of *Danio* species

Adult fish (n=5 each for *D. rerio* (TU), *D. aesculapii*, *D. kyathit*, *D. nigrofasciatus*, *D. tinwini*, *D. albolineatus*, *D. choprae*, *D. erythromicron*, *D. margaritatus*) were euthanized by exposure to buffered 0.5 g/L MS-222 (Tricaine). Skin tissues were dissected in ice-cold PBS and collected using TRIzol (Life Technologies). RNA integrity and quantity were assessed by Agilent 2100 Bioanalyzer. Library preparation (TruSeq stranded mRNA, Illumina; 200 ng per sample) and sequencing (NovaSeq 6000, 2 x 100 bp) were performed by CeGaT GmbH (Tübingen, Germany). RNA-Seq analysis was carried out using the *Danio rerio* GRCz11 genome build for all *Danio* species and STAR aligner with default settings[13]. Differential expression analysis was then carried out using DESeq2[14]. The actual commands used can be found here: https://github.com/najasplus/STAR-deseq2.

519

520 Sequence analysis

521 We found SNPs in the coding region of *Kcnj13* and considered other resources[15],
522 including the latest zebrafish reference genome assembly (GRCz11) and the ENA
523 deposition Zebrafish Genome Diversity (PRJEB20043, Wellcome Trust Sanger).
524 Also, all identified SNPs in the *kcnj13* coding sequence from the Zebrafish Mutation
525 Project were incorporated[16]. The variant calling pipeline for all *Danio* species
526 consisted of GATK 3.8 and 4 and picard[17] from STAR-aligned bam files based on
527 GATK Best-Practices pipeline. The full commands used can be found here:
528 https://github.com/najasplus/rnaseq_variant_calling. Furthermore, variants were also
529 called and checked using SAMtools, mpileup and bcftools[18]. The protein sequence
530 alignment was produced using T-coffee[19] and refined using BOXSHADE (developed
531 by Kay Hofmann and Michael D. Baron, unpublished) and Microsoft Word.

532

533 **Methods References**

534 1 Brand, M., Granato, M. & Nüsslein-Volhard, C. in *Zebrafish: A Practical*
535 *Approach* (eds C. Nüsslein-Volhard & R. Dahm) (Oxford University Press,
536 2002).
537 2 Lister, J. A., Robertson, C. P., Lepage, T., Johnson, S. L. & Raible, D. W.
538 nacre encodes a zebrafish microphthalmia-related protein that regulates
539 neural-crest-derived pigment cell fate. *Development* **126**, 3757-3767 (1999).
540 3 Odenthal, J. *et al.* Mutations affecting xanthophore pigmentation in the
541 zebrafish, Danio rerio. *Development* **123**, 391-398 (1996).
542 4 Krauss, J., Astrinidis, P., Fröhnhofer, H. G., Walderich, B. & Nüsslein-Volhard,
543 C. transparent, a gene affecting stripe formation in Zebrafish, encodes the
544 mitochondrial protein Mpv17 that is required for iridophore survival. *Biol Open*
545 **2**, 703-710, doi:10.1242/bio.20135132 (2013).
546 5 Haffter, P. *et al.* Mutations affecting pigmentation and shape of the adult
547 zebrafish. *Development genes and evolution* **206**, 260-276, doi:DOI
548 10.1007/s004270050051 (1996).

6 Watanabe, M. *et al.* Spot pattern of leopard Danio is caused by mutation in the zebrafish connexin41.8 gene. *EMBO reports* **7**, 893-897, doi:10.1038/sj.embor.7400757 (2006).

7 Irion, U. *et al.* Gap junctions composed of connexins 41.8 and 39.4 are essential for colour pattern formation in zebrafish. *Elife* **3**, e05125, doi:10.7554/eLife.05125 (2014).

8 Parichy, D. M. & Johnson, S. L. Zebrafish hybrids suggest genetic mechanisms for pigment pattern diversification in Danio. *Development genes and evolution* **211**, 319-328 (2001).

9 Parichy, D. M., Elizondo, M. R., Mills, M. G., Gordon, T. N. & Engeszer, R. E. Normal table of postembryonic zebrafish development: staging by externally visible anatomy of the living fish. *Developmental dynamics : an official publication of the American Association of Anatomists* **238**, 2975-3015, doi:10.1002/dvdy.22113 (2009).

10 Irion, U., Krauss, J. & Nüsslein-Volhard, C. Precise and efficient genome editing in zebrafish using the CRISPR/Cas9 system. *Development* **141**, 4827-4830, doi:10.1242/dev.115584 (2014).

11 Meeker, N. D., Hutchinson, S. A., Ho, L. & Trede, N. S. Method for isolation of PCR-ready genomic DNA from zebrafish tissues. *Biotechniques* **43**, 610, 612, 614, doi:10.2144/000112619 (2007).

12 Schindelin, J. *et al.* Fiji: an open-source platform for biological-image analysis. *Nat Methods* **9**, 676-682, doi:10.1038/nmeth.2019 (2012).

13 Dobin, A. & Gingeras, T. R. Mapping RNA-seq Reads with STAR. *Curr Protoc Bioinformatics* **51**, 11 14 11-11 14 19, doi:10.1002/0471250953.bi1114s51 (2015).

14 Love, M. I., Huber, W. & Anders, S. Moderated estimation of fold change and dispersion for RNA-seq data with DESeq2. *Genome Biol* **15**, 550, doi:10.1186/s13059-014-0550-8 (2014).

15 Bowen, M. E., Henke, K., Siegfried, K. R., Warman, M. L. & Harris, M. P. Efficient mapping and cloning of mutations in zebrafish by low-coverage whole-genome sequencing. *Genetics* **190**, 1017-1024, doi:10.1534/genetics.111.136069 (2012).

16 Dooley, C. M. *et al.* Multi-allelic phenotyping--a systematic approach for the simultaneous analysis of multiple induced mutations. *Methods* **62**, 197-206, doi:10.1016/j.ymeth.2013.04.013 (2013).

17 Poplin, R. *et al.* Scaling accurate genetic variant discovery to tens of thousands of samples. *bioRxiv*, 201178, doi:10.1101/201178 (2018).

18 Li, H. *et al.* The Sequence Alignment/Map format and SAMtools. *Bioinformatics* **25**, 2078-2079, doi:10.1093/bioinformatics/btp352 (2009).

19 Notredame, C., Higgins, D. G. & Heringa, J. T-Coffee: A novel method for fast and accurate multiple sequence alignment. *J Mol Biol* **302**, 205-217, doi:10.1006/jmbi.2000.4042 (2000).

Data and code availability

The dataset generated during this study is available at The European Nucleotide Archive (ENA) accession number: pending.

Acknowledgements

We thank all members of the Nüsslein-Volhard laboratory. This work was supported by an ERC Advanced Grant “DanioPattern” (694289) and the Max Planck Society, Germany.

Author information

Affiliations

Department ECNV, Max Planck Institute for Developmental Biology, Tübingen, Baden-Württemberg, Germany

Marco Podobnik, Hans Georg Frohnhöfer, Christopher Dooley, Anastasia Eskova, Christiane Nüsslein-Volhard, Uwe Irion

IBM Systems, IBM Research and Development GmbH, Böblingen, Baden-Württemberg, Germany

Anastasia Eskova

610

611 Contributions

612 All authors were involved in the design of the experiments. M.P., U.I. and H.G.F.
613 performed the experiments. U.I., C.N.V., M.P., H.G.F. and C.D. analysed the data
614 with support of A.E. M.P. made the figures with contributions from U.I. and C.N.V.
615 U.I., C.N.V. and M.P. wrote the manuscript. C.N.V. and U.I. acquired funding.

616

617 Corresponding author

618 Correspondence to Uwe Irion.

619

620 **Ethics declaration**

621 Competing interests

622 The authors declare no competing interests.

623

624

625

626

627

628

629

630

631

632

633

634

635

636

Figures and Figure Legends

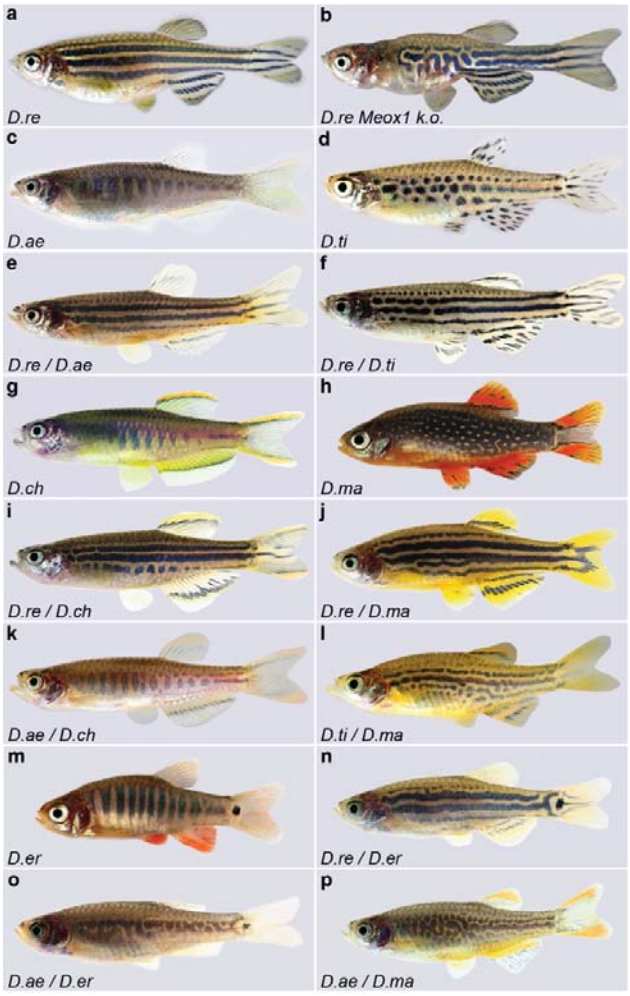

Fig. 1: Colour patterns in *Danio* fish and interspecific hybrids.

a, Colour pattern of zebrafish, *D. rerio* (*D.re*). **b**, *D. rerio Meox1* (*choker*) mutants, which lack a horizontal myoseptum. **c**, *D. aesculapii* (*D.ae*). **d**, *D. tinwini* (*D.ti*). **e**, Interspecific hybrid between *D. rerio* and *D. aesculapii* and, **f**, between *D. rerio* and *D. tinwini*. **g**, *D. choprae* (*D.ch*). **h**, *D. margaritatus* (*D.ma*). **i** Interspecific hybrid between *D. rerio* and *D. choprae*, **j**, and between *D. rerio* and *D. margaritatus*. **k**, Interspecific hybrid between *D. aesculapii* and *D. choprae*. **l**, Interspecific hybrid between *D. tinwini* and *D. margaritatus*. **m**, *D. erythromicron (D. er)*. **n**, Interspecific hybrid between *D. rerio* and *D. erythromicron*. **o**, Interspecific hybrid between *D. aesculapii* and *D. erythromicron.* **p**, Interspecific hybrid between *D. aesculapii* and *D. margaritatus.*

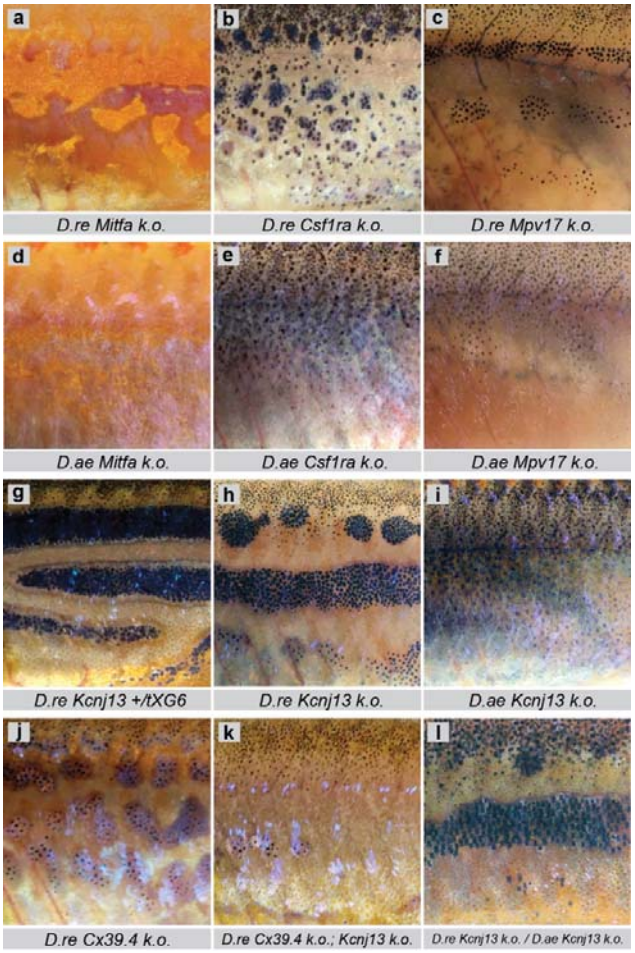

Fig. 2: Mutant phenotypes in *D. rerio*, *D. aesculapii* and their hybrids.

In *D. rerio* loss of one type of pigment cell, **a**, melanophores in *Mitfa* (*nacre*) mutants, **b**, xanthophores in *Csf1ra* (*pfeffer*) mutants, or **c**, iridophores in *Mpv17* (*transparent*) mutants, still permits rudimentary aggregation of dense iridophores (a) or melanophores (b, c). In *D. aesculapii*, **d**, loss of melanophores in *Mitfa* mutants or **e**, loss of xanthophores in *Csf1ra* mutants, abrogate any residual pattern formation. However, **f**, bars still form in *Mpv17* mutants, despite the absence of iridophores. **g**, *D. rerio* heterozygous for the dominant allele $Kcnj13^{tXG6}$/*obelix*. **h**, *D. rerio* homozygous for the loss-of-function allele $Kcnj13^{t24ui}$. **i**, *D. aesculapii* homozygous for a *Kcnj13* loss-of-function allele. **j**, *D. rerio* homozygous for the loss-of-function of Cx39.4. **k**, in *D. rerio* double mutants for *Cx39.4* and *Kcnj13* patterning is completely absent. **l**, interspecific hybrids between *D. rerio* and *D. aesculapii* that are both mutant in *Kcnj13.*

Fig. 3: A reciprocal heterozygosity test to identify *Kcnj13* evolution.

Two interspecific hybrids between *D. rerio* and *D. aesculapii*, which are heterozygous for a *Kcnj13* loss-of-function mutation. **a,** stripes are interrupted in hybrids carrying the mutant allele from *D. rerio* (nick in the blue line representing the zebrafish genome). **b,** hybrids carrying the mutant allele from *D. aesculapii* (nick in the magenta line, representing the *D. aesculapii* genome) are indistinguishable from wild-type hybrids (Fig. 1e).

676

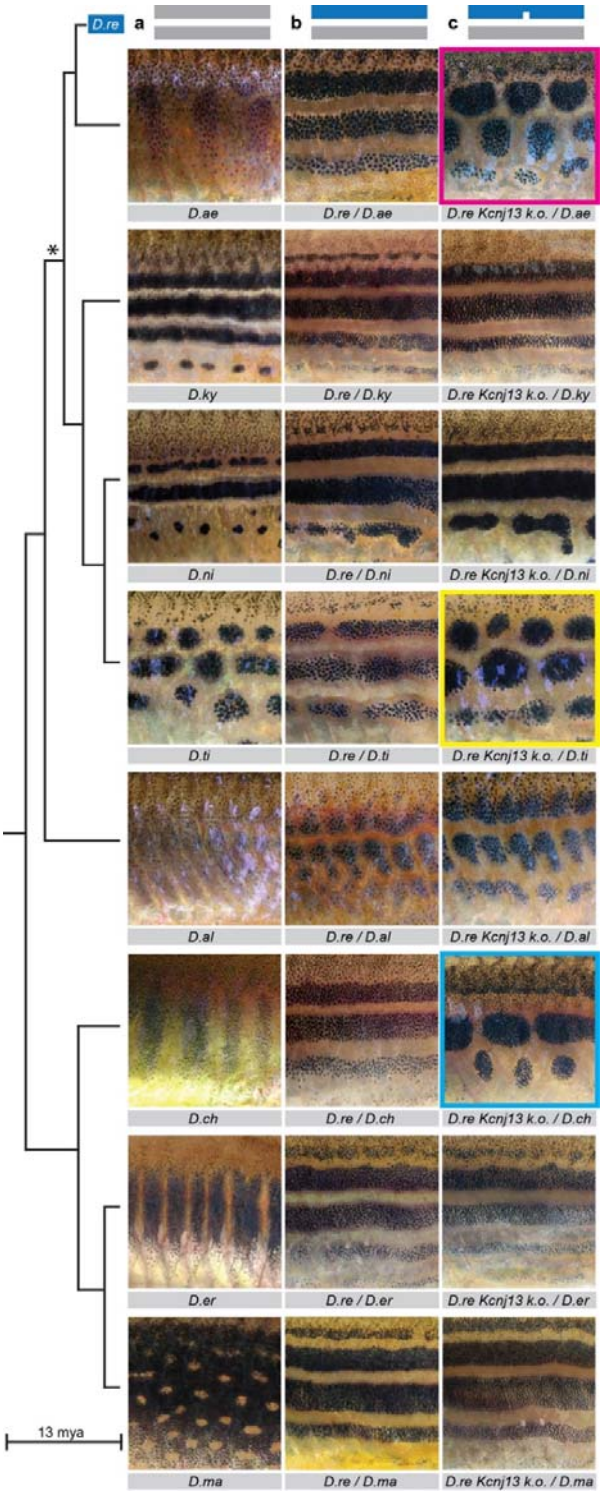

677

678 **Fig. 4: Repeated *Kcnj13* evolution.**

679 **a**, From top to bottom wild-type *Danio* colour patterns (*D. rerio* species group: barred

680 *D. aesculapii*, *D.ae*, the closest relative to *D. rerio*; striped *D. kyathit*, *D.ky*; striped

D. nigrofasciatus, *D.ni*; spotted *D. tinwini*, *D.ti*;) unpatterned *D. albolineatus*, *D.al*; (*D. choprae* species group: barred *D. choprae*, *D.ch*; barred *D. erythromicron*, *D.er*; spotted *D. margaritatus*, *D.ma*). The phylogenetic tree to the left depicts the relationships between the species[1]. The asterisk denotes an uncertainty in the phylogenetic relationships within the *D. rerio* species group. **b**, Hybrids between *D. rerio* (*D.re*) and eight other danios (from top to bottom *D. aesculapii*, *D.ae*, *D. kyathit*, *D.ky, D. nigrofasciatus*, *D.ni*, *D. tinwini*, *D.ti, D. albolineatus*, *D.al, D. choprae*, *D.ch*, *D. erythromicron*, *D.er*, *D. margaritatus*, *D.ma*). **c**, Interspecific hybrids carrying the *Kcnj13* k.o. allele from *D. rerio* and the wild-type allele in the eight species. Pattern defects occur in three cases, *D. rerio Kcnj13* k.o. / *D. aesculapii* (magenta box), *D. rerio Kcnj13* k.o. / *D. tinwini* (yellow box) and *D. rerio Kcnj13* k.o. / *D. choprae* (cyan box). In the other five cases the patterns in heterozygous hybrids do not differ from the striped patterns of wild-type hybrids.

694 **Extended Data Figures, Tables and Legends**

695

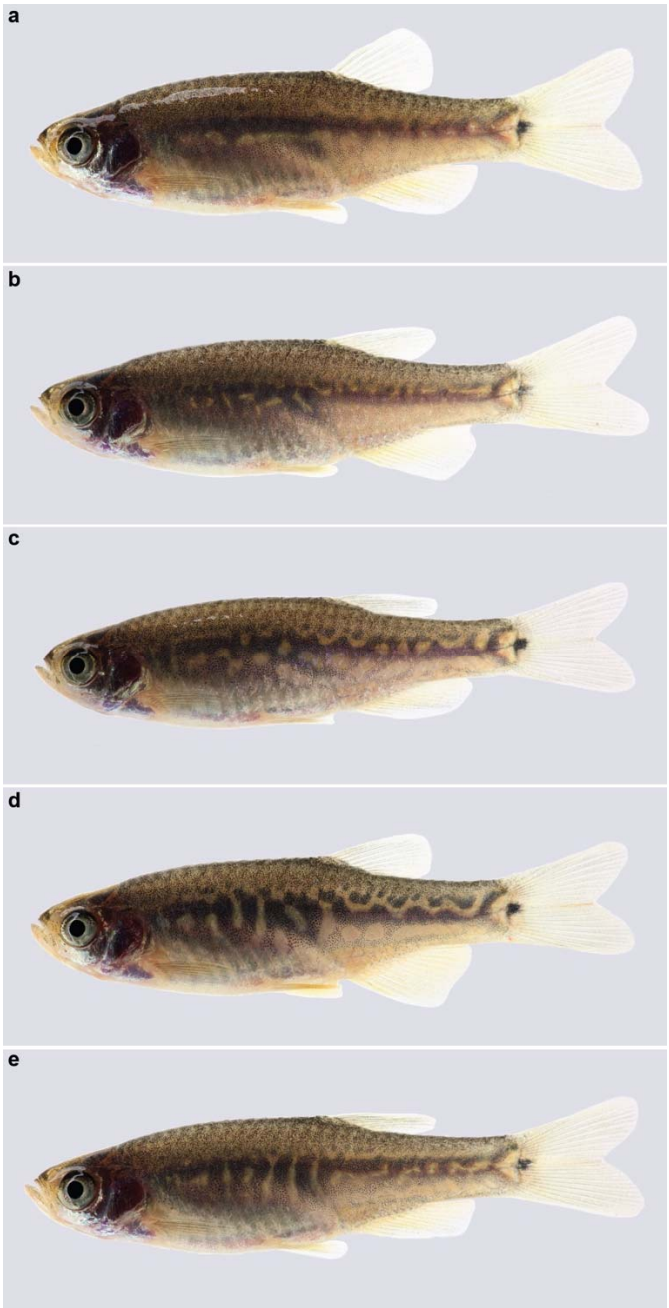

696

697 **Extended Data Fig. 1: Variability of patterns in interspecific hybrids between *D.***
698 ***aesculapii* and *D. erythromicron***

699 Interspecific hybrids between *D. aesculapii* and *D. erythromicron*, **a - e**, show a
700 range of patterns without clear horizontal or vertical orientation.

701

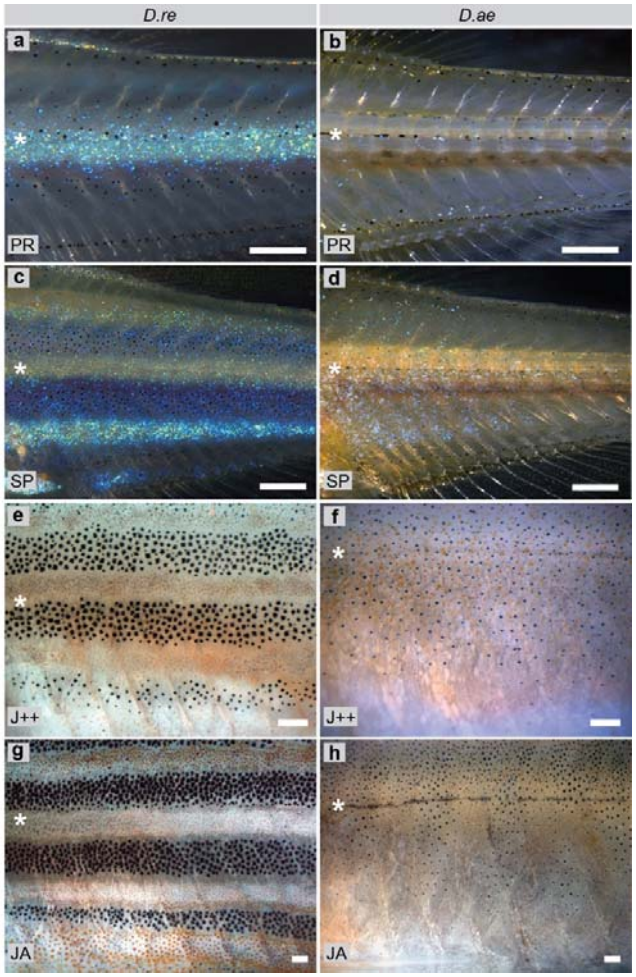

Extended Data Fig. 2: Development of colour patterns in *D. rerio* and *D. aesculapii*.

a, *D. rerio* fish at stage PR. Iridophores (arrowhead) emerge along the horizontal myoseptum (asterisk) to form the first light stripe. **b**, *D aesculapii* fish at stage PR. **c**, *D. rerio* at stage SP. The first light stripe is flanked dorsally and ventrally by dark stripes **d**, *D. aesculapii* at stage SP. Iridophores emerge in a scattered fashion. **e**, *D. rerio* at stage J++. Light stripes are covered by compact xanthophores **f**, *D. aesculapii* at stage J++. Melanophores and xanthophores broadly intermix. **g**, *D. rerio* at stage JA. **h**, *D. aesculapii* at stage JA. Melanophores and xanthophores sort out loosely into vertical bars of low contrast; no dense iridophores are visible between the dark bars. a-d: incident light illumination to highlight iridophores, e-h: bright field illumination to visualise xanthophores and melanophores. Staging according to[2]. PB (pectoral fin bud, 7.2 mm SL). SP (squamation posterior, 9.5 mm

717 SL). J++ (juvenile posterior, 16 mm SL). JA (juvenile-adult, >16 mm SL). Scale bars
718 correspond to 250 µm.
719

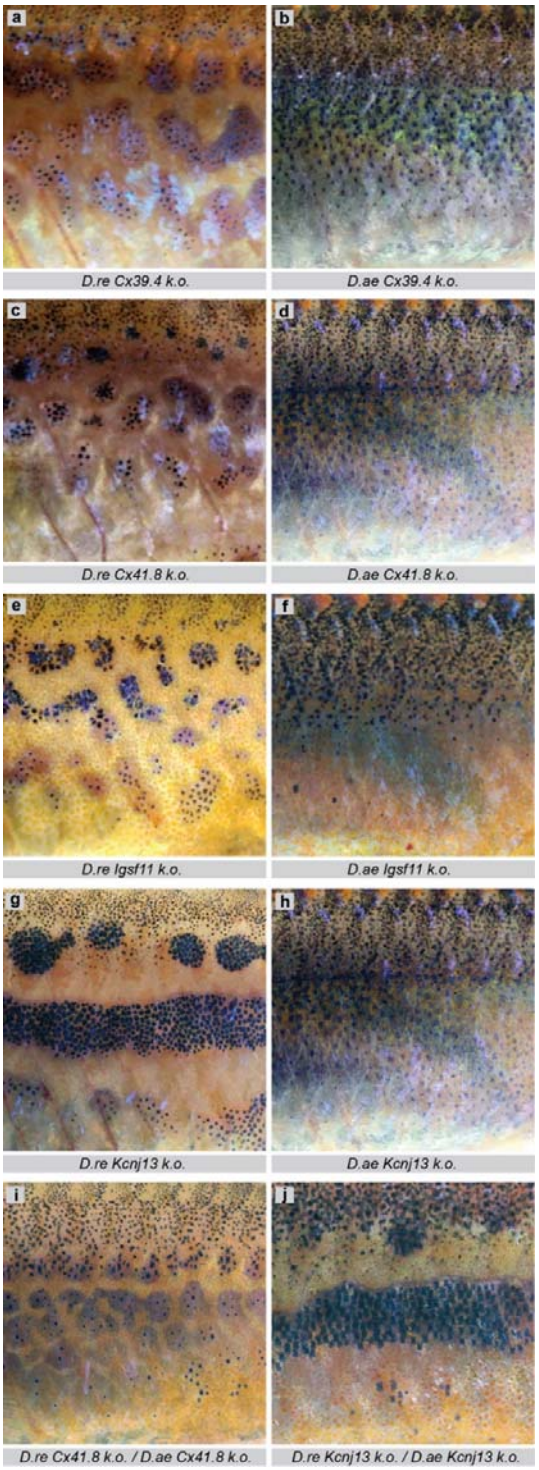

Extended Data Fig. 3: Mutant phenotypes in *D. rerio* and *D. aesculapii* of genes required for heterotypic interactions.

a, *D. rerio* (*D.re*) *Cx39.4* knock-out (k.o.) mutant[3]. **b**, *D. aesculapii* (*D.ae*) *Cx39.4* k.o. mutant. **c**, *D.re Cx41.8* mutant[4,5]. **d**, *D.ae Cx41.8* k.o. mutant. **e**, *D.re Igsf11* k.o.

726 mutant[6]. **f**, *D. ae Igsf11* mutant. **g**, *D. rerio Kcnj13* k.o. mutant[3,4,7]. **h**, *D.ae Kcnj13*
727 k.o. mutant. **i**, Interspecific hybrids between *D.re Cx41.8* and *D.ae Cx41.8* mutants. **j**,
728 Interspecific hybrids between *D.re Kcnj13* and *D.ae Kcnj13* mutants. In all cases,
729 loss-of function (k.o.) alleles were created using CRISPR/Cas9 gene editing.
730

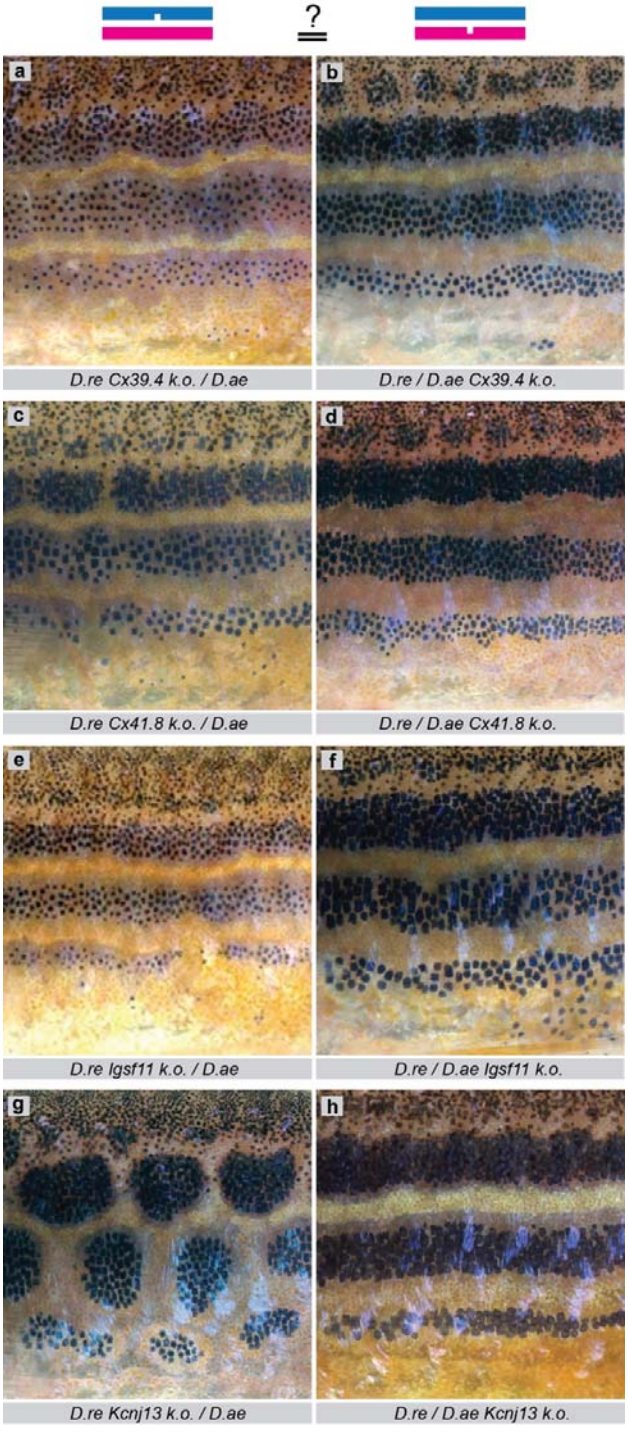

Extended Data Fig. 4: Reciprocal heterozygosity tests identify *Kcnj13* evolution.

Interspecific heterozygous hybrids carrying a mutant allele (nicked bar) from either parental species (blue: *D. rerio*, *D.re*, or magenta: *D. aesculapii*, *D.ae*) in an otherwise identical genetic background. In the cases of **a**/**b**, *Cx39.4*, **c**/**d**, *Cx41.8* and

738 **e**/**f**, *Igsf11* both hybrids show identical phenotypes. In the case of **g**/**h**, *Kcnj13*, the
739 two hybrids show different phenotypes: Interrupted stripes and spots in those
740 carrying the mutant allele from *D. rerio* (g) and a striped pattern in those carrying the
741 mutant allele from *D. aesculapii* (h).
742
743
744

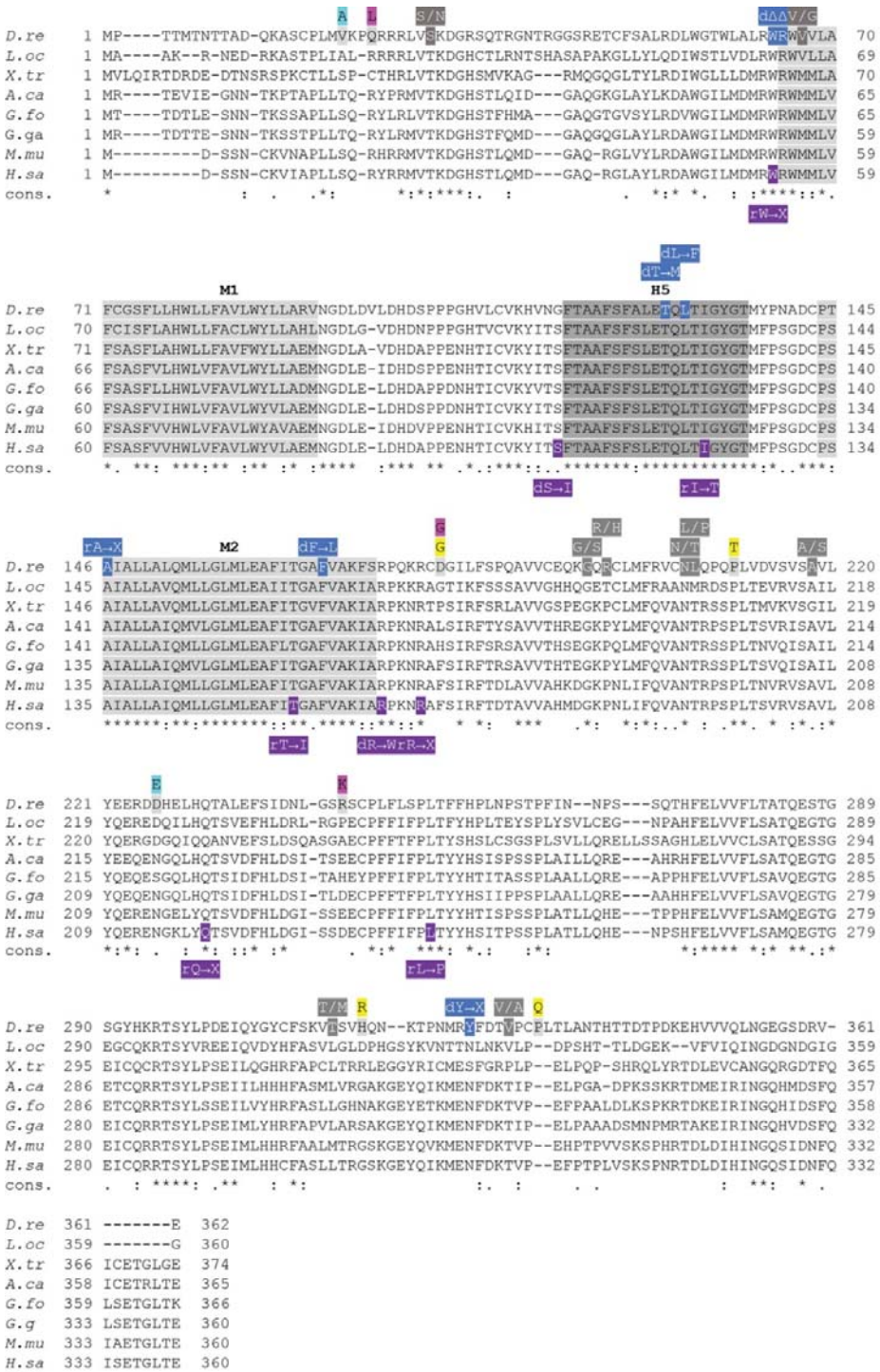

Extended Data Fig. 5: Kcnj13 sequence alignment of vertebrate orthologues. Sequence alignment of Kcnj13 orthologues from different vertebrate species. The two transmembrane domains (M1/M2) are shaded in light grey, the P-Loop (H5) in dark grey. Dominant (d) or recessive (r) mutations are indicated for zebrafish[3,4,7,8]

(blue) and human[9-13] (purple). Positions that are different between *D. rerio* and *D. aesculapii* (magenta), *D. tinwini* (yellow), *D. choprae* (cyan) and polymorphic positions in *D. rerio* (dark grey) are highlighted. Kcnj13 sequences of *Danio rerio* (zebrafish, NP_001039014.1), *Lepisosteus oculatus* (spotted gar, XP_006638004.1), *Xenopus tropicalis* (tropical clawed frog, NP_001096437.1), *Anolis carolinensis* (green anole, XP_016847621.1), *Geospiza fortis* (medium ground finch, XP_005430275.1), *Gallus gallus* (chicken, XP_015132697.1), *Mus musculus* (house mouse, NP_001103697.1) and *Homo sapiens* (human, NP_002233.2).

760

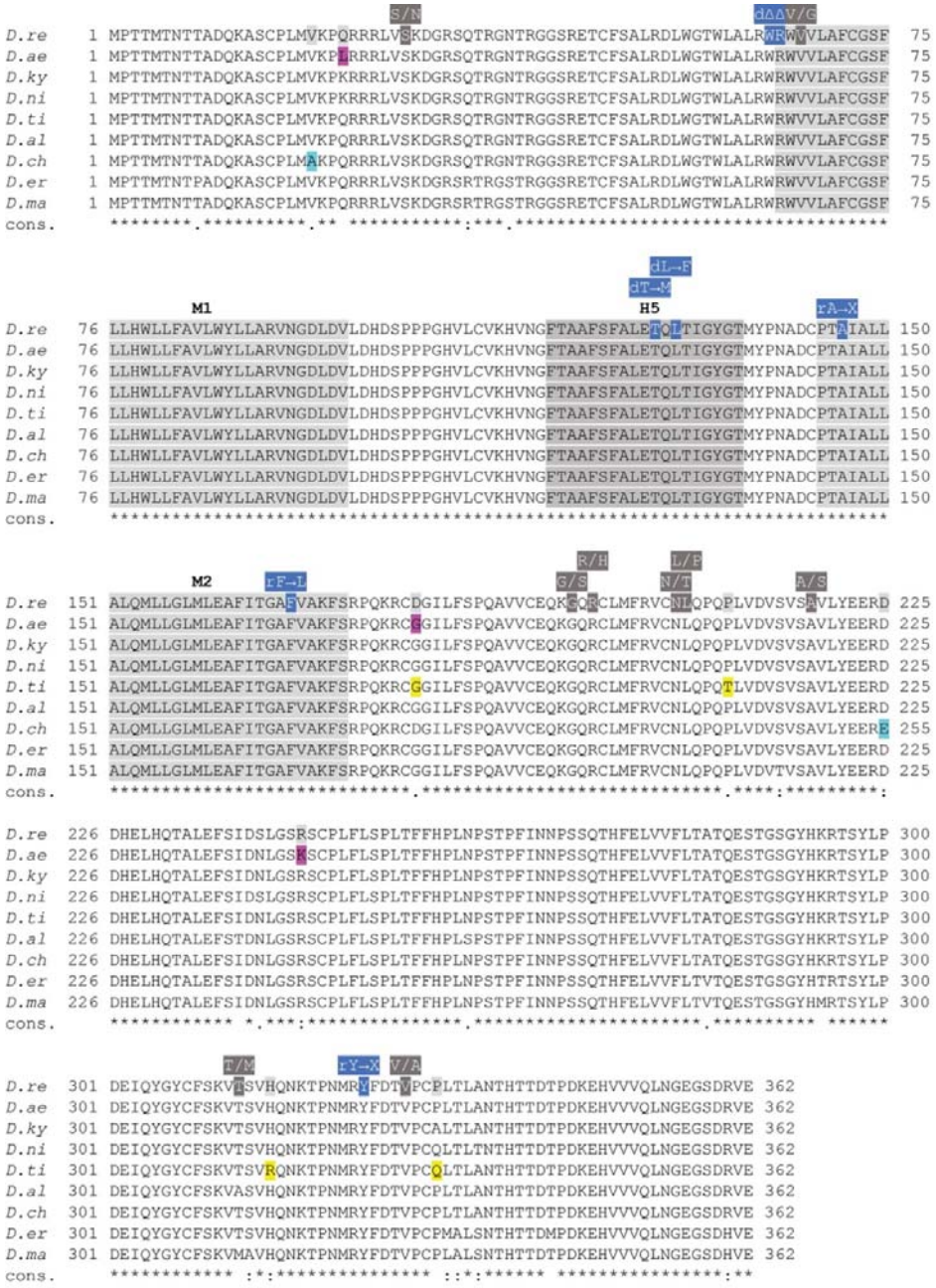

761

762 **Extended Data Fig. 6: Sequence alignment of Kcnj13 orthologues from *Danio***

763 **species.**

764 Kcnj13 sequences from *D. rerio* (*D.re*), *D. aesculapii* (*D.ae*), *D. kyathit* (*D.ky*),

765 *D. nigrofasciatus* (*D.ni*), *D. tinwini* (*D.ti*), *D. albolineatus* (*D.al*), *D. choprae* (*D.ch*),

766 *D. margaritatus* (*D.ma*), *D. erythromicron* (*D.er*). Amino acids evolved between *D.re*

767 and *D.ae* (magenta), *D.ti* (yellow) and *D.ch* (cyan). Dominant (d) or recessive (r)

768 mutations in *D.re Kcnj13*^{3,4,7,8} (blue). Amino acid polymorphisms in *D.re* (dark grey).
769 Transmembrane domains (M1/M2) (light grey blocks) and the P-loop (H5) (dark grey
770 block).
771

772 **Figure References**

773 1 McCluskey, B. M. & Postlethwait, J. H. Phylogeny of zebrafish, a "model
774 species," within Danio, a "model genus". *Mol Biol Evol* **32**, 635-652,
775 doi:10.1093/molbev/msu325 (2015).
776 2 Parichy, D. M., Elizondo, M. R., Mills, M. G., Gordon, T. N. & Engeszer, R. E.
777 Normal table of postembryonic zebrafish development: staging by externally
778 visible anatomy of the living fish. *Developmental dynamics : an official*
779 *publication of the American Association of Anatomists* **238**, 2975-3015,
780 doi:10.1002/dvdy.22113 (2009).
781 3 Irion, U. *et al.* Gap junctions composed of connexins 41.8 and 39.4 are
782 essential for colour pattern formation in zebrafish. *Elife* **3**, e05125,
783 doi:10.7554/eLife.05125 (2014).
784 4 Haffter, P. *et al.* Mutations affecting pigmentation and shape of the adult
785 zebrafish. *Development genes and evolution* **206**, 260-276, doi:DOI
786 10.1007/s004270050051 (1996).
787 5 Watanabe, M. *et al.* Spot pattern of leopard Danio is caused by mutation in
788 the zebrafish connexin41.8 gene. *EMBO reports* **7**, 893-897,
789 doi:10.1038/sj.embor.7400757 (2006).
790 6 Eom, D. S. *et al.* Melanophore migration and survival during zebrafish adult
791 pigment stripe development require the immunoglobulin superfamily adhesion
792 molecule Igsf11. *PLoS genetics* **8**, e1002899,
793 doi:10.1371/journal.pgen.1002899 (2012).
794 7 Iwashita, M. *et al.* Pigment pattern in jaguar/obelix zebrafish is caused by a
795 Kir7.1 mutation: implications for the regulation of melanosome movement.
796 *PLoS genetics* **2**, e197, doi:10.1371/journal.pgen.0020197 (2006).
797 8 Henke, K. *et al.* Genetic Screen for Postembryonic Development in the
798 Zebrafish (Danio rerio): Dominant Mutations Affecting Adult Form. *Genetics*
799 **207**, 609-623, doi:10.1534/genetics.117.300187 (2017).

9 Hejtmancik, J. F. *et al.* Mutations in KCNJ13 cause autosomal-dominant snowflake vitreoretinal degeneration. *Am J Hum Genet* **82**, 174-180, doi:10.1016/j.ajhg.2007.08.002 (2008).

10 Sergouniotis, P. I. *et al.* Recessive mutations in KCNJ13, encoding an inwardly rectifying potassium channel subunit, cause leber congenital amaurosis. *Am J Hum Genet* **89**, 183-190, doi:10.1016/j.ajhg.2011.06.002 (2011).

11 Khan, A. O., Bergmann, C., Neuhaus, C. & Bolz, H. J. A distinct vitreo-retinal dystrophy with early-onset cataract from recessive KCNJ13 mutations. *Ophthalmic Genet* **36**, 79-84, doi:10.3109/13816810.2014.985846 (2015).

12 Perez-Roustit, S. *et al.* Leber Congenital Amaurosis with Large Retinal Pigment Clumps Caused by Compound Heterozygous Mutations in Kcnj13. *Retin Cases Brief Rep* **11**, 221-226, doi:10.1097/ICB.0000000000000326 (2017).

13 Toms, M. *et al.* Missense variants in the conserved transmembrane M2 protein domain of KCNJ13 associated with retinovascular changes in humans and zebrafish. *Exp Eye Res* **189**, 107852, doi:10.1016/j.exer.2019.107852 (2019).

819 **Supplementary Information and Legends**

820

821 Supplementary Tables

822 Table 1 | List of targeted genes.

target	CRISPR target sequence (5'-3')	genotyping
D. aesculapii csf1ra	GGCCTTTAACCTGGTCGGTC	T2143, T2144
D. aesculapii cx39.4	GGACTCACAGCCGGGCTGTT	T2145, T2146
D. aesculapii cx41.8	GAACTTTCTAGAAGAAGTCC	MP92, MP318
D. aesculapii igsf11	GCTGAAAGTACAGGGCAAGA	MP330, MP 331
D. aesculapii kcnj13	TGCTGTATTATGGTACCTGC	T963, T964
D. aesculapii mitfa	GGAGCGCTGGCTCCGGGTCC	T2147, T2148
D. aesculapii mpv17	GGTGCTTTTCTGGGAATAAC	T2149, T2150
D. rerio igsf11	GGACGCAATATAGGAGTGAT	T1449, T1450
D. rerio kcnj13 (1)	GGCAAGCAGCGCGATGGCAG	T2139, T2140
D. rerio kcnj13 (2)	GGCTGGCGCTACGGTGGCGG	T963, T964

823

824 Table 2 | Primer pairs used for the generation of sgRNAs.

target	forward	reverse
D. aesculapii csf1ra	AAACGACCGACCAGGTTAAAGG	TAGGCCTTTAACCTGGTCGGTC
D. aesculapii cx39.4	AAACAACAGCCCGGCTGTGAGT	TAGGACTCACAGCCGGGCTGTT
D. aesculapii mitfa	AAACGGACCCGGAGCCAGCGCT	TAGGAGCGCTGGCTCCGGGTCC
D. aesculapii mpv17	AAACGTTATTCCCAGAAAAGCA	TAGGTGCTTTTCTGGGAATAAC
D. rerio csf1ra	AAACGACCGACCAGGTTAAAGG	TAGGCCTTTAACCTGGTCGGTC
D. rerio igsf11	AAACATCACTCCTATATTGCGT	TAGGACGCAATATAGGAGTGAT
D. rerio kcnj13 (1)	AAACCCGCCACCGTAGCGCCAG	TAGGCTGGCGCTACGGTGGCGG
D. rerio kcnj13 (2)	AAACCTGCCATCGCGCTGCTTG	TAGGCAAGCAGCGCGATGGCAG

825

826 Table 3 | Primers used for genotyping.

primer name	sequence (5'-3')
MP318	AGCTGTGCCCAGAACCAAGA
MP330	CCCCCATGCATTTTATTTGACCA
MP331	CTGAATTCAGAAAGGAGGAGGT
MP92	CTCCCTTCCATTCACACTACC
T963	GAAACTATTCTTGCCGTGACTTG
T964	TCAAACAAACCTGGGTGTGGAC

T1449	TCATCTACCAGAGTGGTCAG
T1450	CCTAAACTTTTGCAGCACAG
T2139	TCAATGGAGACCTGGATGTC
T2140	TGGACCAAAGTGTGAAAGC
T2143	TGCCTGTGTTTATGTGTCG
T2144	AATGACCAAGAAGGATGAGC
T2145	GCCTCTAGGAACATGATTGG
T2146	GCTTCTCATTTCTAGCCCTC
T2147	GGCAACATTGGCGTTATCTC
T2148	TCTCACAGCATTCTGGCAC
T2149	CTGCCGTTTATATCTCCACAG
T2150	GGCTGAAAATTGGCTGATTG

827

828 Table 4 | List of generated mutants.

mutant	mutation	description according to[1]
D. aesculapii Csf1ra^{t31ui}	4 bp deletion	recessive, c.1500_1503delGGTC p.Gly502LysfsX35
D. aesculapii Cx39.4^{t15ui}	8 bp deletion	recessive, c.175_182delAAACAGCC p.Lys59_ArgfsX2
D. aesculapii Cx39.4^{t59ui}	21 bp deletion	recessive, c.168_188delCAACACCAAACAGCCCGGCTG p.Asn57_Cys63del
D. aesculapii Cx41.8^{t18mp}	18 bp deletion	recessive, c.41_58delTCCAGGAGCATTCAACCT p.Val14AlaGlu15_Ser20del
D. aesculapii Igsf11^{t10mp}	1 bp insertion	recessive, c.130dupT p.Leu44PhefsX12
D. aesculapii Igsf11^{t19mp}	11 bp deletion	recessive, c.129_139delCTTGCCCTGTA p.Leu44PhefsX8
D. aesculapii Kcnj13^{t11mp}	4 bp deletion	recessive, c.260_263delACCT p.Tyr87CysfsX27
D. aesculapii Mitfa^{t30ui}	7 bp deletion	recessive, c.194_200delGACCCGG

		p.Gly65GlufsX22
D. aesculapii Mpv17^{t32ul}	4 bp deletion	recessive, c.321_324delAATA p.Ile108LeufsX6
D. rerio Igsf11^{t35ul}	17 bp deletion	recessive, c.412_428delGTGATCGGCCTGACGGT p.Ile138AlafsX19
D. rerio Kcnj13^{dt58ul}	6 bp deletion	dominant, c.190_195delTGGCGG p.Trp64Arg65del
D. rerio Kcnj13^{t24ul}	14 bp insertion	recessive, c.436_437insGATGGAAGATGCTT p.Ala146GlyfsX28

Supplementary Discussion

Kcnj13 functions as a tetramer (Fig. 4d, e), where each subunit contributes two transmembrane helices (M1 and M2, Extended Data Fig. 4) to the formation of the channel pore and a short extracellular loop that folds back to form the pore lining ion selectivity filter (P-loop or H5, Extended Data Fig. 4). The N- and C-termini of the subunits reside in the cytoplasm, where they also contribute to the ion pore, but are mainly involved in gating of the channel (reviewed in[2]). Four dominant *Kcnj13* alleles have been identified in *D. rerio* in several independent forward genetic screens (Extended Data Fig. 4)[3-5]. All of them show broad stripes with irregular interruptions when heterozygous (Fig. 2g) and strong pattern aberrations with fewer, wider and interrupted dark stripes and some mixing of melanophores and xanthophores when homozygous or trans-heterozygous. Three of them carry point mutations affecting H5 or M2[3,4,6], one is the result of a C-terminal truncation (Extended Data Fig. 4)[5]. The point mutations lead to proteins that do not produce functional channels[6] and it has been suggested that the dominant phenotype is caused by a dosage-dependent effect, i.e. haploinsufficiency[7]. To test this possibility we used the CRISPR/Cas9 system and generated a loss of function allele of *Kcnj13* in *D. rerio* which is recessive. The 14 base pair insertion near the end of the first coding exon leads to an early truncation of the protein. Homozygous mutants show a phenotype similar to homozygous mutants for the dominant alleles (Fig. 2h)[3-7]. This shows that the dominant alleles are dominant-negatives, where the mutant proteins inhibit the

function of the wild-type protein in heterozygotes. The generation of this recessive allele allowed us to perform the reciprocal heterozygosity test with *D. aesculapii* as well as interspecific complementation with seven other *Danio* species[8].

Supplementary Information References

1 Ogino, S. *et al.* Standard mutation nomenclature in molecular diagnostics: practical and educational challenges. *J Mol Diagn* **9**, 1-6, doi:10.2353/jmoldx.2007.060081 (2007).

2 Hibino, H. *et al.* Inwardly rectifying potassium channels: their structure, function, and physiological roles. *Physiol Rev* **90**, 291-366, doi:10.1152/physrev.00021.2009 (2010).

3 Haffter, P. *et al.* Mutations affecting pigmentation and shape of the adult zebrafish. *Development genes and evolution* **206**, 260-276, doi:DOI 10.1007/s004270050051 (1996).

4 Irion, U. *et al.* Gap junctions composed of connexins 41.8 and 39.4 are essential for colour pattern formation in zebrafish. *Elife* **3**, e05125, doi:10.7554/eLife.05125 (2014).

5 Henke, K. *et al.* Genetic Screen for Postembryonic Development in the Zebrafish (Danio rerio): Dominant Mutations Affecting Adult Form. *Genetics* **207**, 609-623, doi:10.1534/genetics.117.300187 (2017).

6 Iwashita, M. *et al.* Pigment pattern in jaguar/obelix zebrafish is caused by a Kir7.1 mutation: implications for the regulation of melanosome movement. *PLoS genetics* **2**, e197, doi:10.1371/journal.pgen.0020197 (2006).

7 Maderspacher, F. & Nüsslein-Volhard, C. Formation of the adult pigment pattern in zebrafish requires leopard and obelix dependent cell interactions. *Development* **130**, 3447-3457 (2003).

8 Parichy, D. M. & Johnson, S. L. Zebrafish hybrids suggest genetic mechanisms for pigment pattern diversification in Danio. *Development genes and evolution* **211**, 319-328 (2001).